Journal of Sound and Vibration (1998) **210**(3), 329–350

VIBRATIONS OF BASE PLATES IN ANNULAR CYLINDRICAL TANKS: THEORY AND EXPERIMENTS

M. Amabili

Dipartimento di Ingegneria Industriale, *Università di Parma*, *viale delle Scienze*, *I*-43100 *Parma*, *Italy*

AND

G. Dalpiaz

*Dipartimento di Ingegneria Meccanica** (*DIEM*), *Università di Bologna*, *Bologna*, *Italy*

(*Received* 22 *October* 1996, *and in final form* 18 *September* 1997)

In this paper, the bulging modes (i.e., modes where the walls oscillate moving the liquid) of the flexible bottom annular plate of an otherwise rigid annular cylindrical container are studied. The tank has a vertical axis and is partially filled with liquid, so that the free surface of the liquid is orthogonal to the tank axis. The volume occupied by the liquid is delimited by two coaxial rigid cylinders and the liquid deformation potential is obtained by using variables separation. First, by using the simplifying hypothesis that the mode shapes of the plate in contact with the liquid (wet modes) are the same *in vacuo*, the approach based on the non-dimensionalized added virtual mass incremental (NAVMI) factor is applied, so that all numerical computations can be made non-dimensional. Second, the accuracy of this method is checked by using the Rayleigh–Ritz method, which removes the restrictive hypothesis on the wet mode shapes. Finally, several experimental modal analyses were performed on two different test tanks filled with different water levels in order to verify the accuracy of the theoretical results.

1. INTRODUCTION

Knowledge of the dynamic behaviour is important in the design of off-shore structures, large liquid-fuel rockets and missiles, and heat exchangers for nuclear plants since it influences safety, dynamic stability and control. All these structures are in contact with liquids. Although cylindrical elements are more common in some fields, annular structures are commonly employed in nuclear plants and sometimes in marine applications. Annular tanks have also been proposed for launching vehicles.

The free vibrations of fluid-coupled coaxial cylindrical shells were studied by Au-Yang [1, 2], while the shell vibrations of an annular cylindrical tank were studied by Bauer *et al*. [3] and Zhou [4]. The added mass effect on an annular disc vibrating in fluid was investigated by Kubota and Suzuki [5], but the differentials in the radial direction were neglected and only diametral modes were considered. This study is, therefore, mainly applicable to plates having a ratio between the inner and outer radius close to one (rings). Recently, Amabili *et al*. [6] analytically solved the problem of the free vibrations of an annular plate placed into the hole of an infinite rigid plate (infinite baffle) and in contact with an unbounded liquid on one side. The effect of a finite fluid depth on this problem was investigated by Amabili [7]. The vibration of an elastic membrane bottom of a rigid

*Dipartimento di Ingegneria delle Costruzioni Meccaniche, Mulleari, Aeronautiche e di Metallurgia.

0022–460X/98/080329 + 22 $25.00/0/sv971280

annular tank partially filled with liquid was studied by Tsui and Small [8]. No studies on vibrations of annular bottom plates of rigid annular tanks partially filled with liquid have been found in the open literature by the authors.

In this paper, attention is focused on the bulging modes of the flexible bottom annular plate of an otherwise rigid annular cylindrical container. It is worthy to remember that partially liquid-filled tanks have two families of modes: the sloshing and the bulging ones. Sloshing modes are caused by the oscillation of the liquid free surface, e.g., they are excited by the rigid body movement of the container; these modes can also be affected by the flexibility of the container but are characteristic of rigid tanks. Obviously they disappear for empty tanks. On the contrary, bulging modes are related to vibrations of the tank walls (bottom plate and shell) that move the liquid. This family of modes is due to the flexibility of the structure, disappears in the case of rigid walls, but is also present for empty flexible containers.

The tank studied has a vertical axis and is partially filled with liquid, so that the free surface of the liquid is orthogonal to the tank axis. The volume occupied by the liquid is delimited by two coaxial rigid cylinders and the liquid deformation potential can be obtained by using variables separation. The effects of the free surface waves on the dynamic pressure at the free surface, the superficial tension and the gravity effects are neglected [9], so that the plate vibrations, with only bulging modes considered, are studied by using a simplified theory. In fact, it is well known that the effect of the free surface waves is low on bulging modes of structures which are not extremely flexible [9]. As a consequence, the non-dimensionalized added virtual mass incremental (NAVMI) factor approach, already successfully used for circular plates in references [6, 7, 10–14] is applied. In particular, Amabili [13] applied a similar method to study base circular plates of cylindrical tanks; however, in the present study the geometry is more complicated. All computations can be made non-dimensional and the natural frequencies of the annular plate in contact with the liquid can be obtained directly from those *in vacuo* by using the actual plate boundary conditions. This a relevant computational simplification in respect to other existing theoretical approaches. Some interesting work on fluid-loaded plates and membranes has been reported, e.g., in references [15–45] and this provides several solutions of different problems. Moreover, due to their non-dimensional form, NAVMI factors can be computed once and for all. The proposed approach is based on the Rayleigh quotient for coupled vibrations [46, 47] and on the hypothesis that the dry (*in vacuo*) and wet (in liquid) mode shapes of the plate remain unchanged (based on the assumed modes method). The accuracy of this approach is checked by using the Rayleigh–Ritz method [48], which removes the restrictive hypothesis on the wet mode shapes. In particular, the wet mode shapes are expanded in a series by using the dry mode shapes as admissible functions.

The Rayleigh–Ritz approach allows one to exceed the limits of the assumed modes method, while retaining a remarkable simplicity of computation, in respect to other analytical techniques already applied to this kind of problem. Moreover, non-dimensional results can be given for engineering applications.

The present study can be considered an extension to the classical problem of the vibrations of circular bottom plates of otherwise rigid cylidrical tanks partially filled with a liquid [13, 18–25, 32, 35, 37–39]. This classic problem can be obtained as a special case of an annular tank, when the inner radius becomes zero. In fact, in this case, a simpler solution of the equation of motion satisfies the boundary conditions for free vibrations in vacuum.

In order to check the accuracy of the proposed theory, several experimental modal analyses were performed on two different test tanks filled with different water levels. Results obtained by the numerical simulation of the free vibration characteristics of the

tank bottom are satisfactorily compared to data obtained by the experiments. These results give a validation of the hypotheses and the theory used in the present work.

The theory is applicable to engineering problems and the NAVMI factor approach has the advantage of presenting the results as tables of non-dimensional factors that can be quickly employed in design. In the case that the entire tank must be considered flexible, the approach used is still useful to study the whole structure if a sub-structuring method, like the artificial spring method, is used.

2. PLATE VIBRATIONS IN VACUUM

Consider a thin annular plate vibrating *in vacuo* having thickness h, mass density ρ_P, inner radius a_1, and outer radius a_2. The plate is assumed to be made of linearly elastic, homogeneous and isotropic material. Moreover, the effects of shear deformation and rotary inertia are neglected. A polar co-ordinate system $(O; r, \theta)$ is introduced, with the pole O placed on the plate centre. The equation of motion for transverse displacement, w, of this plate is [49]

$$D\nabla^4 w + \rho_P h(\partial^2 w/\partial t^2) = 0, \tag{1}$$

where $D = Eh^3/[12(1 - \nu^2)]$ is the flexural rigidity of the plate; ν and E are the Poisson ratio and the Young's modulus, respectively. In addition, ∇^4 is the iterated Laplace operator; the Laplace operator, in polar co-ordinates, is $\nabla^2 = \partial^2/\partial r^2 + (1/r)\partial/\partial r + (1/r^2)\partial^2/\partial\theta^2$. In the case of uniform constraints along the edge, the solution takes the following form [49, 50]

$$w(r, \theta, t) = W_{mn}(r) \cos(m\theta) f(t), \tag{2}$$

where

$$W_{mn}(r) = A_{mn} \mathrm{J}_m\left(\frac{\lambda_{mn} r}{a_2}\right) + B_{mn} \mathrm{Y}_m\left(\frac{\lambda_{mn} r}{a_2}\right) + C_{mn} \mathrm{I}_m\left(\frac{\lambda_{mn} r}{a_2}\right) + D_{mn} \mathrm{K}_m\left(\frac{\lambda_{mn} r}{a_2}\right), \tag{3}$$

$$f(t) = \mathrm{e}^{\mathrm{i}\omega t} \tag{4}$$

in which m and n represent the number of nodal diameters and circles, respectively. A_{mn}, B_{mn}, C_{mn} and D_{mn} are the mode shape constants determined by the boundary conditions, J_m and Y_m are the Bessel functions of first and second kind, I_m and K_m are the modified Bessel functions of first and second kind, and λ_{mn} is the frequency parameter also determined by the boundary conditions. For circular plates $B_{mn} = D_{mn} = 0$ as a consequence that equation (3) must be limited for $r = 0$. The frequency parameter, λ_{mn}, is related to the circular frequency, ω_{mn}, of the plate *in vacuo* by

$$\omega_{mn} = (\lambda_{mn}^2/a_2^2)\sqrt{D/(\rho_P h)}. \tag{5}$$

For the Poisson ratio $\nu = 0{\cdot}3$, the values of λ_{mn} are tabulated in reference [51] with three significant digits for nine different boundary conditions. In reference [6] λ_{mn} with six significant digits for three different edge constraints as well as mode shape constants of axisymmetric modes are given.

In the present work the following normalization criterion has been used for the mode shape constants:

$$\int_a^1 W_{mn}^2(\rho)\rho \, \mathrm{d}\rho = 1. \tag{6}$$

Here $a = a_1/a_2$ is the ratio between the inner and outer radius and $\rho = r/a_2$ is the non-dimensional radial co-ordinate.

3. LIQUID-PLATE INTERACTION

The study is that of the free vibrations of an annular bottom plate of an otherwise rigid annular tank filled with an inviscid and incompressible liquid, movement of which is due only to the plate vibrations. In this section, the dry and wet mode shapes of the plate are assumed to be equal. The liquid deformations are described by the spatial deformation potential Φ_{mn}, which satisfies the Laplace equation

$$\nabla^2 \Phi_{mn}(x, r, \theta) = 0, \tag{7}$$

where the Laplace operator in cylindrical co-ordinates is $\nabla^2 = \partial^2/\partial x^2 + \partial^2/\partial r^2 + (1/r)\partial/\partial r + (1/r^2)\partial^2/\partial\theta^2$. The cylindrical co-ordinate system $(O; x, r, \theta)$ has the pole O placed where the tank axis intersects the middle plane of the plate. The conditions of impermeable walls at the liquid–rigid tank interfaces for a non-caviting liquid are

$$(\partial \Phi_{mn}/\partial r)_{r=a_1} = 0, \qquad (\partial \Phi_{mn}/\partial r)_{r=a_2} = 0. \tag{8, 9}$$

The free liquid surface condition is described by the zero dynamic pressure condition at $x = H$ [9, 46, 48, 52],

$$(\Phi_{mn})_{x=H} = 0, \tag{10}$$

where H is the level of the liquid in the annular container (see Figure 1). This condition is obtained by neglecting the contribution of the free surface waves and superficial tension to the dynamic pressure of the liquid at $x = H$. This simplification does not induce significant errors for tanks when only bulging modes are studied. Studying the shell

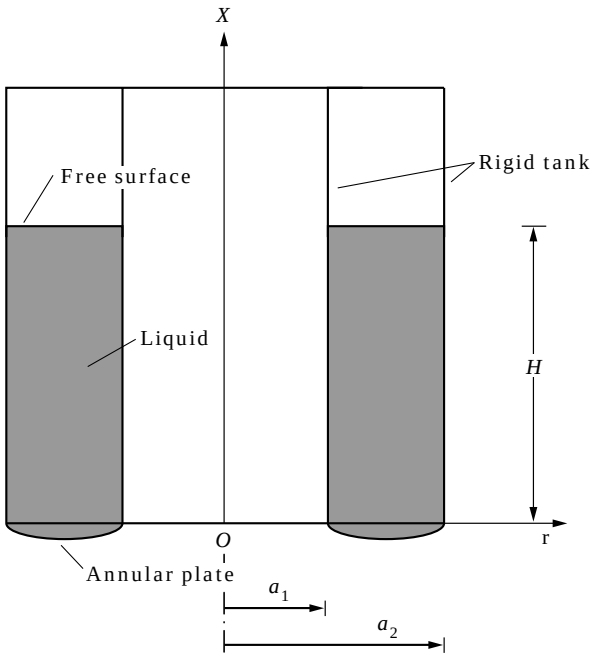

Figure 1. Rigid annular tank with flexible bottom plate.

vibrations, Kondo [53] discussed this phenomenon, observing that the heights of the free surface waves for bulging modes of circular cylindrical tanks are so small that they almost coincide with the undisturbed liquid level. This simplification is the same as that obtained by considering the case of zero gravity (without superficial tension) and does not constrain the vertical velocity of the liquid. As a consequence of this condition, the free surface does not exhibit an intrinsic capability to oscillate; thus, the liquid free surface is not subjected to a restoring force once it has moved, and sloshing modes cannot be studied.

At the liquid–flexible plate interface, the contact is assured by

$$(\partial \Phi_{mn}/\partial x)_{x=0} = -w(r, \theta, t)_{t=0}. \tag{11}$$

The spatial distribution of the liquid deformation potential, for asymmetric modes ($m \geqslant 1$), is given by

$$\Phi_{mn}(x, r, \theta) = \cos(m\theta) \sum_{k=0}^{\infty} h_{mnk} \left[\mathrm{J}_m\left(\epsilon_{mk} \frac{r}{a_2}\right) + \gamma_{mk}\, \mathrm{Y}_m\left(\epsilon_{mk} \frac{r}{a_2}\right) \right]$$

$$\times \left[\cosh\left(\epsilon_{mk} \frac{x}{a_2}\right) - \sinh\left(\epsilon_{mk} \frac{x}{a_2}\right) \Big/ \tanh\left(\epsilon_{mk} \frac{H}{a_2}\right) \right], \tag{12}$$

where h_{mnk} are appropriate constants. For axisymmetric modes ($m = 0$), Φ_{mn} is given by

$$\Phi_{0n}(x, r) = g_{0n0}(x - H) + \sum_{k=0}^{\infty} h_{0nk} \left[\mathrm{J}_0\left(\epsilon_{0k} \frac{r}{a_2}\right) + \gamma_{0k}\, \mathrm{Y}_0\left(\epsilon_{0k} \frac{r}{a_2}\right) \right]$$

$$\times \left[\cosh\left(\epsilon_{0k} \frac{x}{a_2}\right) - \sinh\left(\epsilon_{0k} \frac{x}{a_2}\right) \Big/ \tanh\left(\epsilon_{0k} \frac{H}{a_2}\right) \right]. \tag{13}$$

Equations (12) and (13) satisfy only the free surface condition (10). The conditions (8) and (9) require that

$$\mathrm{J}'_m(\epsilon_{mk}) + \gamma_{mk}\, \mathrm{Y}'_m(\epsilon_{mk}) = 0, \qquad \mathrm{J}'_m(\epsilon_{mk}\, a) + \gamma_{mk}\, \mathrm{Y}'_m(\epsilon_{mk}\, a) = 0. \tag{14}$$

From the first equation of the system one obtains

$$\gamma_{mk} = -\mathrm{J}'_m(\epsilon_{mk})/\mathrm{Y}'_m(\epsilon_{mk}). \tag{15}$$

Upon introducing the function F_m,

$$F_m(\epsilon_{mk}\, \rho) = \mathrm{J}_m(\epsilon_{mk}\, \rho)\mathrm{Y}'_m(\epsilon_{mk}) - \mathrm{J}'_m(\epsilon_{mk})\mathrm{Y}_m(\epsilon_{mk}\, \rho), \tag{16}$$

substituting expression (15) into the second equation of system (14) and using equation (16) yields

$$F'_m(\epsilon_{mk}\, a) = 0, \tag{17}$$

where $F'_m = \partial F_m/\partial r$. Equation (17) is equivalent to system (14) when $a \neq 0$; when $a = 0$ (circular plate) only the first equation of system (14) must be used and γ_{mk} equals zero. Therefore ϵ_{mk} are the roots of equation (17).

By using the orthogonality of functions F_m, proved in the Appendix, one can write

$$\int_a^1 \rho F_m(\epsilon_{mk}\, \rho) F_m(\epsilon_{mh}\, \rho)\, \mathrm{d}\rho = \delta_{kh}\, \alpha_{mk}, \tag{18}$$

where δ_{kh} is the Kronecker delta. Calling $\tilde{h}_{mnk} = h_{mnk} / \mathrm{Y}'_m(\epsilon_{mk})$, one obtains the following expression for Φ_{mn} for asymmetric modes:

$$\Phi_{mn}(x, r, \theta) = \cos(m\theta) \sum_{k=0}^{\infty} \tilde{h}_{mnk} F_m(\epsilon_{mk} r/a_2) \left[\cosh\left(\epsilon_{mk} \frac{x}{a_2}\right) - \sinh\left(\epsilon_{mk} \frac{x}{a_2}\right) \Big/ \tanh\left(\epsilon_{mk} \frac{H}{a_2}\right) \right]. \tag{19}$$

Then, one requires that Φ_{mn} satisfies the last boundary condition, equation (11):

$$\cos(m\theta) \sum_{k=0}^{\infty} \tilde{h}_{mnk} F_m(\epsilon_{mk} r/a_2) \frac{\epsilon_{mk}}{a_2 \tanh(\epsilon_{mk} H/a_2)} = W_{mn}(r) \cos(m\theta). \tag{20}$$

Condition (20) is used to evaluate the constants $\tilde{h}_{mnk}$:

$$\tilde{h}_{mnk} = \frac{a_2 \tanh(\epsilon_{mk} H/a_2)}{\epsilon_{mk}} \frac{\displaystyle\int_a^1 W_{mn}(a_2 \rho) F_m(\epsilon_{mk} \rho) \rho \, \mathrm{d}\rho}{\displaystyle\int_a^1 F_m^2(\epsilon_{mk} \rho) \rho \, \mathrm{d}\rho} = \frac{a_2 \tanh(\epsilon_{mk} H/a_2)}{\epsilon_{mk}} \frac{\beta_{mnk}}{\alpha_{mk}}, \tag{21}$$

where

$$\beta_{mnk} = \int_a^1 W_{mn}(a_2 \rho) F_m(\epsilon_{mk} \rho) \rho \, \mathrm{d}\rho.$$

For axisymmetric modes, the boundary condition (11) yields

$$-g_{0n0} + \sum_{k=0}^{\infty} \tilde{h}_{0nk} F_0(\epsilon_{0k} r/a_2) \frac{\epsilon_{0k}}{a_2 \tanh(\epsilon_{0k} H/a_2)} = W_{0n}(r). \tag{22}$$

Therefore one has

$$g_{0n0} = -2 \int_a^1 W_{0n}(a_2 \rho) \rho \, \mathrm{d}\rho, \tag{23}$$

and the constants $\tilde{h}_{0nk}$ are given by equation (21) computed for $m = 0$.

4. NAVMI FACTORS

4.1. FORMULATION

If one applies Green's theorem to the harmonic function Φ_{mn}, the reference kinetic energy of the liquid can be computed as a boundary integral [47, 54]:

$$T_L^* = \frac{1}{2} \rho_L \iiint_V \nabla \Phi_{mn} \nabla \Phi_{mn} \, \mathrm{d}V = -\frac{1}{2} \rho_L \iint_{\partial V} \Phi_{mn} (\partial \Phi_{mn} / \partial n) \, \mathrm{d}S, \tag{24}$$

where V is the liquid volume, ∂V is the boundary of the volume V, and n is the direction normal to the boundary oriented inwards to the liquid region. Due to equations (8–10), only the integration over the plate surface gives a non-zero result; therefore, the reference kinetic energy of the liquid, for asymmetric modes ($m \geqslant 1$) is given by

$$T_L^* = -\frac{1}{2}\rho_L \int_0^{2\pi}\int_{a_1}^{a_2} \Phi_{mn}(0, r, \theta)\frac{\partial \Phi_{mn}}{\partial x}(0, r, \theta) r \, \mathrm{d}r \, \mathrm{d}\theta$$

$$= \frac{1}{2}\rho_L a_2^3 \psi_m \sum_{k=0}^{\infty} \frac{\beta_{mnk}}{\alpha_{mk}} \frac{\tanh(\epsilon_{mk} H/a_2)}{\epsilon_{mk}} \int_a^1 W_{mn}(a_2 \rho) F_m(\epsilon_{mk} \rho) \rho \, \mathrm{d}\rho$$

$$= \frac{1}{2}\rho_L a_2^3 \psi_m \sum_{k=0}^{\infty} \frac{\beta_{mnk}^2}{\alpha_{mk}} \frac{\tanh(\epsilon_{mk} H/a_2)}{\epsilon_{mk}}, \qquad \psi_m = \begin{cases} 2\pi & \text{for } m = 0 \\ \pi & \text{for } m > 0. \end{cases} \tag{25}$$

The reference kinetic energy of the liquid for axisymmetric modes ($m = 0$) is given by

$$T_L^* = \frac{1}{2}\rho_L a_2^3 \psi_m \left[\frac{H}{a_2}\frac{g_{0n0}^2}{2} + \sum_{k=0}^{\infty} \frac{\beta_{0nk}^2}{\alpha_{0k}} \frac{\tanh(\epsilon_{0k} H/a_2)}{\epsilon_{0k}}\right]. \tag{26}$$

The reference kinetic energy of the plate, by using the orthogonality of the dry (equal to wet) mode shapes, is easily obtained

$$T_P^* = \frac{1}{2}\rho_P h \int_{a_1}^{a_2} W_{mn}^2(r)\cos^2(m\theta) r \, \mathrm{d}r \, \mathrm{d}\theta = \frac{1}{2}\rho_P h \psi_m a_2^2 \int_a^1 W_{mn}^2(a_2 \rho)\rho \, \mathrm{d}\rho = \frac{1}{2}\rho_P h \psi_m a_2^2, \tag{27}$$

where the normalization criterion, equation (6), was used.

One can now introduce the non-dimensionalized added virtual mass incremental (NAVMI) factors that are given by the non-dimensional ratio between the reference kinetic energies of the liquid and the plate. These factors relate the natural frequencies of free vibration in liquid, f_L, to natural frequencies in vacuum, f_V, by using the formula $f_L = f_V / \sqrt{1 + \Gamma_{mn}(\rho_L a)/(\rho_P h)}$ [11]. This formula is easily obtained by applying the Rayleigh quotient to the problem. The NAVMI factors for asymmetric modes ($m \geqslant 1$) are given by

$$\Gamma_{mn} = \frac{T_L^*}{T_P^*}\frac{\rho_P h}{\rho_L a_2} = \sum_{k=0}^{\infty} \frac{\beta_{mnk}^2}{\alpha_{mk}} \frac{\tanh(\epsilon_{mk} H/a_2)}{\epsilon_{mk}}; \tag{28}$$

NAVMI factors for axisymmetric modes ($m = 0$) are

$$\Gamma_{0n} = \frac{H}{a_2}\frac{g_{0n0}^2}{2} + \sum_{k=0}^{\infty} \frac{\beta_{0nk}^2}{\alpha_{0k}} \frac{\tanh(\epsilon_{0k} H/a_2)}{\epsilon_{0k}}. \tag{29}$$

4.2. NUMERICAL RESULTS

The NAVMI factors Γ_{mn} are numerically obtained from equations (28) and (29). These factors are given in Tables 1 and 2 for annular plates clamped at both edges for the ratios

TABLE 1

NAVMI factors for annular plates clamped at both edges; $a = 0{\cdot}3$

H/a_2	n	$m = 0$	$m = 1$	$m = 2$	$m = 3$
0·1	0	0·15565	0·092804	0·090770	0·087719
0·1	1	0·080650	0·079116	0·077554	0·075123
0·1	2	0·077591	0·065729	0·064639	0·062928
0·1	3	0·055006	0·054347	0·053631	0·052503
0·3	0	0·40656	0·20988	0·18572	0·15905
0·3	1	0·13010	0·12443	0·11716	0·10727
0·3	2	0·12616	0·089938	0·085451	0·079725
0·3	3	0·068821	0·066805	0·064695	0·061748
0·5	0	0·60887	0·27082	0·21840	0·17379
0·5	1	0·14583	0·13619	0·12491	0·11156
0·5	2	0·16088	0·099332	0·090826	0·082360
0·5	3	0·074506	0·070887	0·067302	0·063178
0·7	0	0·78031	0·30082	0·22865	0·17661
0·7	1	0·15504	0·14129	0·12712	0·11232
0·7	2	0·19099	0·10399	0·092532	0·082870
0·7	3	0·078120	0·072805	0·068096	0·063449
1	0	1·0011	0·31794	0·23224	0·17720
1	1	0·16318	0·14414	0·12787	0·11248
1	2	0·23066	0·10665	0·093130	0·082978
1	3	0·081376	0·073892	0·068372	0·063505
2	0	1·6419	0·32442	0·23289	0·17725
2	1	0·17598	0·14522	0·12801	0·11249
2	2	0·34846	0·10766	0·093239	0·082987
2	3	0·086640	0·074303	0·068422	0·063510

$a = 0{\cdot}3$ and 0·5, respectively. Different filling ratio H/a_2 and modes having up to three internal nodal diameters and circles are considered in these two tables. Obviously the NAVMI factors increase with the filling ratio so that the natural frequencies decrease. A comparison of the data presented in Tables 1 and 2 shows that the factors for plates with $a = 0{\cdot}3$ are larger than those for plates with $a = 0{\cdot}5$. An interesting phenomenon is also observed for axisymmetric modes of annular plates clamped at both edges: when the filling ratio is high enough (not lower than 0·5 for $a = 0{\cdot}3$ and 0·3 for $a = 0{\cdot}5$) the NAVMI factors do not decrease with the number of nodal circles, as they usually do for an unbounded liquid domain [6]. In fact, axisymmetric modes having an even number of nodal circles give a larger movement of the liquid mass centre than modes with an odd number of nodal circles (asymmetric modes, $m > 0$, give no movement of the liquid mass centre). Therefore, for these modes the liquid influence on the system is larger than for other modes. This phenomenon is evident for the axisymmetric mode with two nodal circles ($m = 0, n = 2$) that presents NAVMI factors higher with respect to those of the axisymmetric mode with one or three nodal circles.

In Table 3, the NAVMI factors for annular plates simply supported at both edges, with $a = 0{\cdot}3$ and $v = 0{\cdot}3$, are reported. The corresponding frequency parameters and mode shape constants are given in Table 4. A comparison of Tables 1 and 3, that are both relative to plates with the same ratio $a = 0{\cdot}3$, show that NAVMI factors are higher for clamped plates than for simply supported plates. Finally, annular plates simply supported at the outer edge and free at the inner edge, with $a = 0{\cdot}3$ and $v = 0{\cdot}3$, are considered in Tables 5 and 6. All these data are given because, due to their non-dimensional nature, they can be used in design and research.

TABLE 2

NAVMI factors for annular plates clamped at both edges; $a = 0{\cdot}5$

H/a_2	n	$m = 0$	$m = 1$	$m = 2$	$m = 3$
0·1	0	0·14048	0·088467	0·087147	0·085063
0·1	1	0·069288	0·068732	0·067989	0·066804
0·1	2	0·063344	0·053443	0·053005	0·052302
0·1	3	0·042517	0·042306	0·042053	0·041644
0·3	0	0·34432	0·18409	0·16982	0·15169
0·3	1	0·097247	0·095241	0·092226	0·087904
0·3	2	0·099227	0·069121	0·066882	0·063897
0·3	3	0·050437	0·049713	0·048766	0·047433
0·5	0	0·49314	0·22303	0·19503	0·16530
0·5	1	0·10485	0·10136	0·096499	0·090478
0·5	2	0·12545	0·074882	0·070678	0·066005
0·5	3	0·053314	0·051996	0·050330	0·048353
0·7	0	0·61416	0·23659	0·20154	0·16769
0·7	1	0·10809	0·10341	0·097552	0·090906
0·7	2	0·14760	0·076893	0·071662	0·066377
0·7	3	0·054579	0·052778	0·050727	0·048511
1	0	0·77660	0·24176	0·20336	0·16813
1	1	0·11014	0·10418	0·097845	0·090986
1	2	0·17800	0·077661	0·071937	0·066446
1	3	0·055394	0·053077	0·050838	0·048541
2	0	1·2941	0·24282	0·20359	0·16817
2	1	0·11347	0·10434	0·097883	0·090992
2	2	0·27581	0·077818	0·071972	0·066451
2	3	0·056757	0·053138	0·050852	0·048543

5. RAYLEIGH–RITZ SOLUTION

5.1. FORMULATION

The Rayleigh–Ritz method [55] is applied to eliminate the restrictive hypothesis that dry and wet modes have the same shape. All other hypotheses, previously introduced, are

TABLE 3

NAVMI factors for annular plates simply supported at both edges; $a = 0{\cdot}3$ *and* $v = 0{\cdot}3$

H/a_2	n	$m = 0$	$m = 1$	$m = 2$	$m = 3$
0·1	0	0·12053	0·047974	0·050027	0·052913
0·1	1	0·042013	0·040075	0·036746	0·032109
0·3	0	0·32579	0·10502	0·10271	0·099637
0·3	1	0·10178	0·094112	0·080196	0·063068
0·5	0	0·49968	0·12894	0·11936	0·10965
0·5	1	0·13211	0·11818	0·094850	0·070170
0·7	0	0·65694	0·13728	0·12367	0·11141
0·7	1	0·14497	0·12661	0·098663	0·071427
1	0	0·88138	0·14046	0·12488	0·11174
1	1	0·15218	0·12983	0·099728	0·071664
2	0	1·6152	0·14111	0·12503	0·11177
2	1	0·16106	0·13049	0·099866	0·071681

TABLE 4

Frequency parameters and mode shape constants for annular plates simply supported at both edges; $a = 0{\cdot}3$ and $\nu = 0{\cdot}3$

m	n	λ_{mn}	A_{mn}	B_{mn}	C_{mn}	D_{mn}
0	0	4·591207	0·880140	−1	0·00242160	−0·742943
0	1	9·040835	0·796941	0·363571	$-8{\cdot}18918 \times 10^{-6}$	−1
1	0	4·828781	0·565809	1	−0·00167875	0·457191
1	1	9·199745	0·611594	−0·820965	$-8{\cdot}48430 \times 10^{-6}$	−1
2	0	5·502127	1	0·431159	−0·00087463	0·187963
2	1	9·665253	0·325297	1	$6{\cdot}07719 \times 10^{-6}$	0·665953
3	0	6·473757	1	0·135945	−0·000350001	0·0587031
3	1	10·40202	1	0·754967	$4{\cdot}02879 \times 10^{-6}$	0·419376

retained. The wet mode shapes W, by using the unknown parameters q_n and the admissible functions W_{mn}, can be described by

$$W(r, \theta) = \cos(m\theta) \sum_{n=0}^{\infty} q_n W_{mn}(r), \tag{30}$$

where W_{mn} is given by equation (3). In equation (30) the eigenfunctions of the annular plate vibrating *in vacuo* are assumed as admissible functions; in fact, dry mode shapes are quite similar to wet mode shapes. The trial functions W_{mn} are linearly independent and constitute a complete set.

Using the principle of superposition, and considering that the plate deflection is given by the sum in equation (30), yields the deformation potential of the liquid, Φ, calculated at the liquid-plate interface ($x = 0$) as

$$\Phi(0, r, \theta) = \sum_{n=0}^{\infty} q_n \Phi_{mn}(0, r, \theta). \tag{31}$$

TABLE 5

NAVMI factors for annular plates simply supported at the outer edge and free at the inner edge; $a = 0{\cdot}3$ and $\nu = 0{\cdot}3$

m	n	$H/a_2 = 0{\cdot}1$	$H/a_2 = 0{\cdot}3$	$H/a_2 = 0{\cdot}5$	$H/a_2 = 0{\cdot}7$	$H/a_2 = 1$
0	0	0·14725	0·37022	0·54997	0·70802	0·92056
0	1	0·084804	0·18269	0·25510	0·30983	0·37019
0	2	0·070207	0·11822	0·13943	0·15505	0·17381
1	0	0·088044	0·19223	0·24395	0·26919	0·28357
1	1	0·069559	0·12521	0·15313	0·16704	0·17499
2	0	0·089913	0·18654	0·22036	0·23100	0·23472
2	1	0·070538	0·11209	0·12378	0·12742	0·12869
3	0	0·088575	0·16695	0·18432	0·18768	0·18839

TABLE 6

Frequency parameters and mode shape constants for annular plates simply supported at the outer edge and free at the inner edge; $a = 0{\cdot}3$ and $\nu = 0{\cdot}3$

m	n	λ_{mn}	A_{mn}	B_{mn}	C_{mn}	D_{mn}
0	0	2·159647	2·82848	−0·109921	−0·154460	0·807153
0	1	6·086234	4·06457	2·95393	0·00118885	9·93240
0	2	10·36667	1·20098	−6·61921	0·0000147858	−56·0205
0	3	14·76906	8·01086	−1·10986	$-1{\cdot}49848 \times 10^{-7}$	−267·844
0	4	19·21184	3·69607	8·47952	$1{\cdot}54588 \times 10^{-9}$	−1198·73
1	0	3·579934	3·25667	−0·449711	−0·0251672	0·794987
1	1	6·770313	4·82793	−0·927146	0·000601226	9·48944
1	2	10·68826	5·69738	3·46801	−0·0000107666	53·2456
1	3	14·95956	0·691184	−8·03343	$-1{\cdot}26083 \times 10^{-7}$	−255·069
1	4	19·34321	8·94154	−2·32103	$1{\cdot}37978 \times 10^{-9}$	−1147·52
2	0	4·910799	3·96371	−0·547221	−0·00663620	−0·0855986
2	1	8·064606	4·85442	−1·49597	0·000180045	5·62635
3	0	6·226935	4·58626	−0·381816	−0·00215876	−0·249744

To perform numerical computations for each fixed m value, only a finite number N of terms must be considered in the previous sum. For this purpose, a vector $\mathbf{q}$ of the unknown parameters is introduced:

$$\mathbf{q} = \begin{Bmatrix} q_0 \\ q_1 \\ \vdots \\ q_{N-1} \end{Bmatrix}. \tag{32}$$

To make the formulae more compact, the constant $\sigma = a_2^2 \psi_m$ is introduced. With this notation, the reference kinetic energy of the liquid is given by

$$T_L^* = \frac{1}{2} \sigma \rho_L a_2 \, \mathbf{q}^{\mathrm{T}} \mathbf{M}_L \, \mathbf{q}, \tag{33}$$

where the $N \times N$ symmetric NAVMI matrix $\mathbf{M}_L$ for asymmetric modes ($m \geqslant 1$) is

$$M_{L_{ij}} = \sum_{k=0}^{\infty} \frac{\beta_{mik} \, \beta_{mjk}}{\alpha_{mk} \, \epsilon_{mk}} \tanh(\epsilon_{mk} \, H/a_2), \quad i, j = 0, 1, \ldots, N-1, \tag{34}$$

and for symmetric modes ($m = 0$), it is defined by

$$M_{L_{ij}} = \frac{g_{0i0} \, g_{0j0}}{2} \frac{H}{a_2} + \sum_{k=0}^{\infty} \frac{\beta_{0ik} \, \beta_{0jk}}{\alpha_{0k} \, \epsilon_{0k}} \tanh(\epsilon_{0k} \, H/a_2), \quad i, j = 0, 1, \ldots, N-1. \tag{35}$$

The acronym NAVMI matrix stands for the non-dimensionalized added virtual mass incremental matrix which in fact describes the inertial effect of the liquid on modes. Therefore, this is the extension of the NAVMI factors to the Rayleigh–Ritz approach. Moreover, the NAVMI factors are the diagonal elements of the NAVMI matrix.

The reference kinetic energy of the plate, by using the normalization introduced in equation (6) and the orthogonality of the dry mode shapes, is given by

$$T_P^* = \frac{1}{2} \sigma \rho_P \, h \mathbf{q}^{\mathrm{T}} \mathbf{I} \mathbf{q}, \tag{36}$$

where $\mathbf{I}$ is the $N \times N$ identity matrix. The maximum potential energy of the system, considering an incompressible liquid having a zero dynamic pressure on the free surface, coincides with that of the plate and can be computed as the sum of the reference kinetic energies of the dry eigenfunctions

$$V_P = \frac{1}{2}\sigma(D/a_2^4)\mathbf{q}^{\mathrm{T}}\mathbf{P}\mathbf{q}, \tag{37}$$

where $\mathbf{P}$ is the $N \times N$ diagonal matrix given by

$$P_{ij} = \delta_{ij}\lambda_{mi}^4, \tag{38}$$

and δ_{ij} is the Kronecker delta. In order to find natural frequencies and wet mode shapes of the plate vibrating in contact with the liquid, the Rayleigh quotient for coupled vibration in an inviscid and imcompressible liquid [46] is used: $V_P/(T_P^* + T_L^*)$. Minimizing the Rayleigh quotient with respect to the unknown parameters q_n, one obtains

$$(D/a_2^4)\mathbf{P}\mathbf{q} - \Lambda^2(\rho_P h\mathbf{I} + \rho_L a_2 \mathbf{M}_L)\mathbf{q} = 0, \tag{39}$$

where Λ is the circular frequency of the wet plate. Equation (39) is a Galerkin equation and gives an eigenvalue problem. It is convenient to introduce the following non-dimensional constants:

$$\Omega^2 = \Lambda^2(a_2^4/D)\rho_P h, \qquad \mu = (\rho_L a_2)/(\rho_P h). \tag{40, 41}$$

Ω and μ are called the wet frequency parameter and the density-thickness correction factor, respectively. Now equation (39) can be rewritten in the following non-dimensional form:

$$\mathbf{P}\mathbf{q} - \Omega^2(\mathbf{I} + \mu\mathbf{M}_L)\mathbf{q} = 0. \tag{42}$$

It is interesting to see that, if the NAVMI matrix $\mathbf{M}_L$ is diagonal, the system of equations (42) is uncoupled. In this case, the approximate solutions given in section 4 become exact.

5.2. NUMERICAL RESULTS

The eigenvalue problem given by equation (42) is solved by using the computer program *Mathematica* [56]. Only five terms of the series were used, but they assure a good accuracy for the first two or three modes. The NAVMI matrix $\mathbf{M}_L$ for axisymmetric modes ($m = 0$) of annular plates clamped at both edges and with $a = 0{\cdot}3$ and $H/a_2 = 1$ is

$$\begin{bmatrix} 1{\cdot}0011 & 0{\cdot}15950 & -0{\cdot}36653 & 0{\cdot}10499 & 0{\cdot}22974 \\ 0{\cdot}15950 & 0{\cdot}16318 & -0{\cdot}075464 & 0{\cdot}046429 & 0{\cdot}049505 \\ -0{\cdot}36653 & -0{\cdot}075464 & 0{\cdot}23066 & -0{\cdot}050576 & -0{\cdot}10648 \\ 0{\cdot}10499 & 0{\cdot}046429 & -0{\cdot}050576 & 0{\cdot}081376 & 0{\cdot}033570 \\ 0{\cdot}22974 & 0{\cdot}049505 & -0{\cdot}10648 & 0{\cdot}033570 & 0{\cdot}10953 \end{bmatrix}. \tag{43}$$

The matrix is not diagonal, so that the system of equations giving the modes is not uncoupled. Only in the first row of the matrix is there a large prevalence of one element (the first) on the others, so, in this case, only the first (fundamental) axisymmetric mode is accurately estimated by the NAVMI factor method. The wet frequency parameters Ω are given for this case as a function of the density-thickness correction factor μ in Figure 2. Curves relative to the first three axisymmetric modes are given. The circular frequencies of this plate are obtained by using equation (41) and Figure 2. The percentage of error committed by using the NAVMI factors solution instead of the Rayleigh–Ritz solution given by equation (42) is plotted in Figure 3 as a function of μ for the same case. It is clear that the fundamental mode is accurately estimated by the approximated (NAVMI

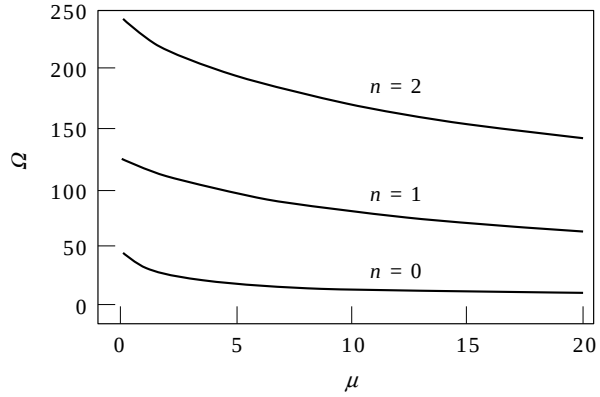

Figure 2. Wet frequency parameters Ω of axisymmetric modes ($m = 0$) of annular plates clamped at both edges with $a = 0{\cdot}3$ and $H/a_2 = 1$, versus the density-thickness correction factor μ. Curves relating to the first three modes are given.

factor) solution and that the errors increase with μ. Even the wet mode shapes have been investigated by using equation (42). In Figure 4, the dry and wet mode shapes are plotted along a radius for $\mu = 10$, modes with up to two nodal circles being considered. It is clear that, as well as natural frequency, the mode shape of the fundamental mode ($m = 0$; $n = 0$) shows little changes.

The NAVMI matrix for axisymmetric modes ($m = 0$) of annular plates simply supported at the outer edge and free at the inner edge and with a $a = 0{\cdot}3$, $v = 0{\cdot}3$ and $H/a_2 = 0{\cdot}2$ is

$$\begin{bmatrix} 0{\cdot}26737 & -0{\cdot}10363 & -0{\cdot}022879 & 0{\cdot}043196 & -0{\cdot}018210 \\ -0{\cdot}10363 & 0{\cdot}13860 & 0{\cdot}051850 & -0{\cdot}0096054 & 0{\cdot}027903 \\ -0{\cdot}022879 & 0{\cdot}051850 & 0{\cdot}10130 & -0{\cdot}030340 & 0{\cdot}0081956 \\ 0{\cdot}043196 & -0{\cdot}0096054 & -0{\cdot}030340 & 0{\cdot}074475 & -0{\cdot}019755 \\ -0{\cdot}018210 & 0{\cdot}027903 & 0{\cdot}0081956 & -0{\cdot}019755 & 0{\cdot}057550 \end{bmatrix}. \quad (44)$$

In this case, due to the lower value of the filling ratio H/a_2, the NAVMI matrix is diagonally dominant: that is, the elements on the diagonal are larger than the off-diagonal ones. As a consequence, the NAVMI factors method estimates well the natural frequencies.

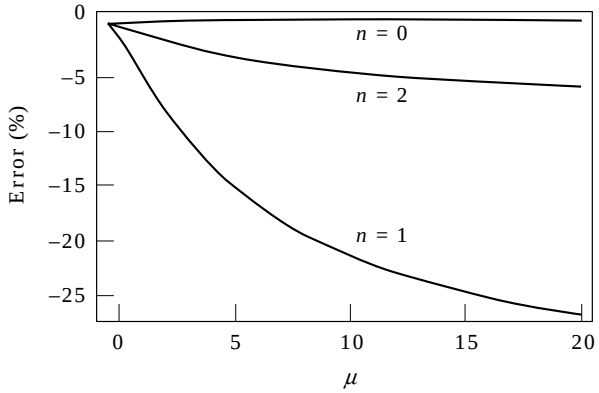

Figure 3. The percentage of error of the assumed modes solution with respect to the Rayleigh–Ritz result as function of μ for annular plates clamped at both edges; $m = 0$, $a = 0{\cdot}3$ and $H/a_2 = 1$.

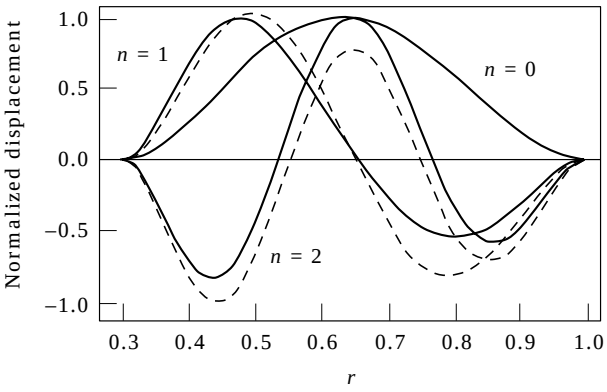

Figure 4. Comparison of dry (dashed lines) and wet (solid lines) modes for annular plates clamped at both edges; $m = 0$, $a = 0{\cdot}3$, $\mu = 10$ and $H/a_2 = 1$.

The NAVMI matrix for the same case, when the filling ratio is increased to $H/a_2 = 1$, is

$$\begin{bmatrix} 0{\cdot}92056 & -0{\cdot}46459 & -0{\cdot}21390 & 0{\cdot}18692 & -0{\cdot}12700 \\ -0{\cdot}46459 & 0{\cdot}37019 & 0{\cdot}17401 & -0{\cdot}098624 & 0{\cdot}095634 \\ -0{\cdot}21390 & 0{\cdot}17401 & 0{\cdot}17381 & -0{\cdot}080158 & 0{\cdot}046361 \\ 0{\cdot}18692 & -0{\cdot}098624 & -0{\cdot}080158 & 0{\cdot}11119 & -0{\cdot}047180 \\ -0{\cdot}12700 & 0{\cdot}095634 & 0{\cdot}046361 & -0{\cdot}047180 & 0{\cdot}078477 \end{bmatrix}. \quad (45)$$

In this case, the matrix is no longer diagonally dominant. The wet frequency parameters Ω are given as a function of the density-thickness correction factor μ in Figure 5. For this case also the first three axisymmetric modes are considered. The percentage of error committed by using the NAVMI factors solution instead of the Rayleigh–Ritz solution is plotted in Figure 6 as a function of μ. It is easily verified that the fundamental mode ($m = 0, n = 0$) is accurately estimated by the approximated (NAVMI factor) solution. In

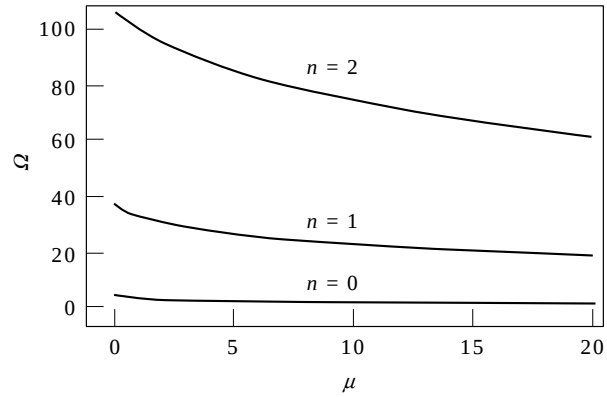

Figure 5. Wet frequency parameters Ω of axisymmetric modes ($m = 0$) of annular plates simply supported at the outer edge and free at the inner edge with $a = 0{\cdot}3$, $v = 0{\cdot}3$ and $H/a_2 = 1$, versus the density-thickness correction factor μ. Curves relating to the first three modes are given.

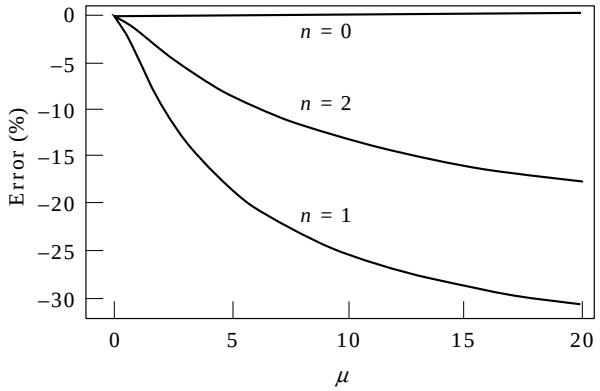

Figure 6. The percentage of error of the assumed modes solution with respect to the Rayleigh–Ritz result as a function of μ for annular plates simply supported at the outer edge and free at the inner edge; $m = 0$, $a = 0{\cdot}3$, $v = 0{\cdot}3$ and $H/a_2 = 1$.

Figure 7, the dry and wet mode shapes are plotted along a radius for $\mu = 10$, modes having up to two nodal circles being considered.

Natural frequencies obtained by using the NAVMI factors and the Rayleigh–Ritz method are compared to the theoretical ones given by Chiba [38] for bulging modes of a clamped circular bottom plate, where the effects of both the free surface waves on the dynamic pressure and the in-plane stress of the plate were considered. Results of Chiba [38] refer to a steel plate having radius $a_2 = 0{\cdot}144$ m, thickness $h = 0{\cdot}002$ m, Young's modulus $E = 206$ GPa, Poisson's ratio $v = 0{\cdot}25$, mass density $\rho_P = 7850$ kg m^{-3} in contact with water having $\rho_L = 1000$ kg m^{-3}. In Table 7, the natural frequencies of the first three axisymmetric modes of the plate are reported for three different filling ratios: $H/a_2 = 0{\cdot}1$, $0{\cdot}5$ and 1. It is clear that the results of the Rayleigh–Ritz method always match well the Chiba results (the Chiba results were obtained by the pesent authors by using a graph reported in reference [38], so that small differences with the actual results computed by Chiba could occur), confirming that the applied free surface condition (zero dynamic pressure at $x = H$) is correct when studying bulging modes. This result confirms what was found by Kondo [53] for circular shells: i.e., that the effect of free surface waves on bulging modes is almost negligible. Moreover, the simple NAVMI factor approach gives quite

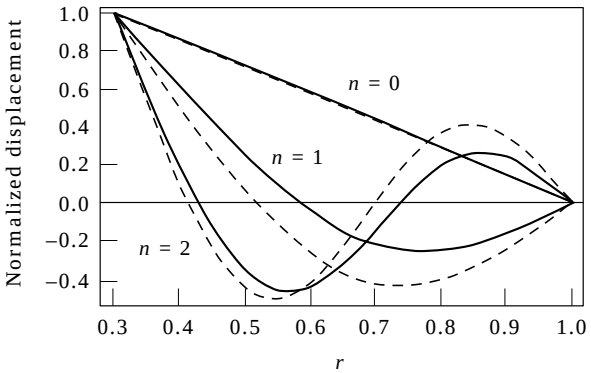

Figure 7. Comparison of dry (dashed lines) and wet (solid lines) modes for annular plates simply supported at the outer edge and free at the inner edge; $m = 0$, $a = 0{\cdot}3$, $v = 0{\cdot}3$, $\mu = 10$ and $H/a_2 = 1$.

TABLE 7

Comparison of natural frequencies (Hz) of the first three axisymmetric modes of the circular plate studied by Chiba [38] *and obtained by using three different theories: the NAVMI factors, the Rayleigh–Ritz method and the theory presented by Chiba in reference* [38]

		Natural frequencies (Hz)		
Mode	H/a_2	NAVMI	Rayleigh–Ritz	Chiba [38]
1st	0·1	176·6	176·8	177
1st	0·5	109·9	114·5	110
1st	1	85·1	91·7	92
2nd	0·1	698·1	700·7	694
2nd	0·5	530·2	547·3	540
2nd	1	485·9	519·8	520
3rd	0·1	1602	1609·7	1620
3rd	0·5	1377	1408·7	1410
3rd	1	1313	1385	1390

good results, especially for the fundamental mode and for small values of the ratio H/a_2. In fact, it was previously found that, when the ratio H/a_2 increases, the accuracy of the NAVMI factor approach decreases.

5.3. ADDITIONAL EFFECTS: IN-PLANE LOAD AND WINKLER FOUNDATION

By using the Rayleigh–Ritz method shown in section 5.1, it is possible to include in the study some additional effects, such as the influence of a uniform in-plane load applied to the annular plate and a Winkler elastic foundation under the plate, without significant complication of the theory. The in-plane load gives an additional potential energy during the plate vibration that must be added to the numerator of the Rayleigh quotient. The maximum potential energy connected with this phenomenon is [57]

$$V_L = \frac{1}{2} L \int_0^{2\pi} \int_{a_1}^{a_2} \{[\partial W/\partial r]^2 + [(1/r)\,(\partial W/\partial \theta)]^2\} r \, \mathrm{d}r \, \mathrm{d}\theta, \tag{46}$$

where L is the uniform in-plane tensile load (N/m). It is to be noted that a compressive load ($L < 0$) gives a negative energy which decreases the natural frequencies. The elastic foundation gives an additional potential energy of which the maximum value is

$$V_F = \frac{1}{2} k_1 \int_0^{2\pi} \int_{a_1}^{a_2} W^2 r \, \mathrm{d}r \, \mathrm{d}\theta, \tag{47}$$

where k_1 is the stiffness of the foundation (N m^{-3}). The matrices related to equations (46, 47) used in the eigenvalue problem can be easily obtained by using the method shown in section 5.1.

6. EXPERIMENTS

6.1. EXPERIMENTAL EQUIPMENT AND PROCEDURE

Two different tanks were constructed to perform the experimental tests. The first specimen (see Figure 8) was designed in order to obtain an annular tank with cylindrical walls that could be considered rigid and a bottom annular plate that could be considered

simply supported on the outer border and free on the inner border. This specimen was an annular tank with an annular bottom plate made of low carbon steel (UNI Fe P 11 MG according to the Italian standards) having thickness $h = 1{\cdot}5$ mm, inner radius $a_1 = 0{\cdot}03$ m and outer radius $a_2 = 0{\cdot}1$ m. The material properties were Young's modulus 206 GPa, mass density 7800 kg/m^3 and Poisson's ratio $v = 0{\cdot}3$. The tank was composed of an external PVC (polyvinyl chloride) pipe glued to the bottom plate; the pipe edge at the shell-plate joint was tapered in order to simulate a simple support and have a negligible bending moment at the joint. To this pipe was glued a very stiff support made of steel that constrains the movement of the tank; this constraint gave practically zero displacement to the plate outer edge at low frequencies. An inner PVC pipe was rigidly connected to

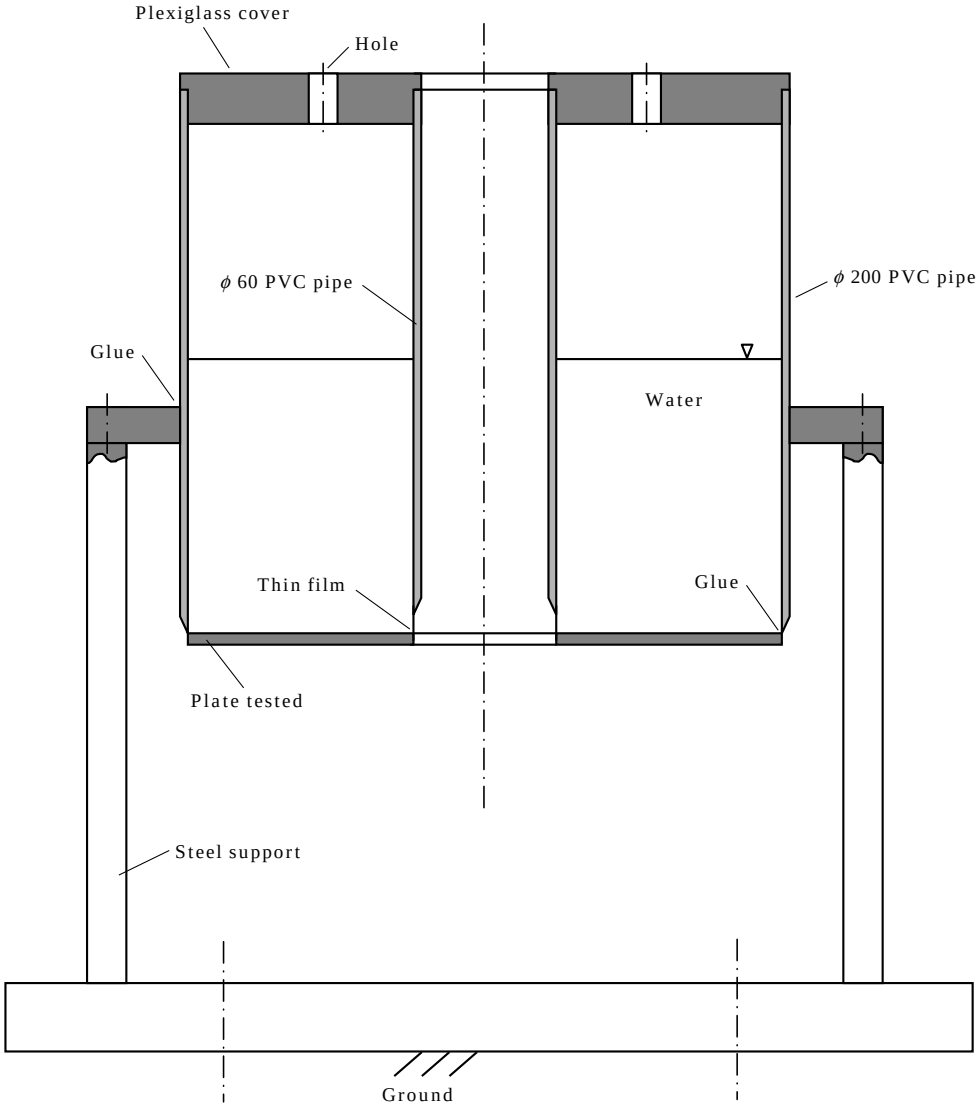

Figure 8. Schematic diagram of the annular tank tested.

the outer pipe by using a thick Plexiglas annular plate having two holes for the introduction of liquids into the tank. A very thin film was then used to connect the inner pipe to the inner edge of the annular plate to keep the water and to give no constraint at the inner edge of the plate. The two pipes were chosen with a flexural stiffness different from that of the plates in order to have a negligible dynamic coupling of the bottom plate and the tank cylindrical walls. Moreover, the pipe material assured a quite high damping to the pipe modes. Then, the tank was partially filled with water, having mass density $\rho_L = 10^3$ kg m^{-3}.

The second tested specimen was designed in order to obtain a circular tank with cylindrical walls that could be considered rigid and a bottom circular plate that could be considered simply supported. It was a tank similar to the previous one but having a circular plate as the bottom, and therefore without the inner pipe and the Plexiglas cover. In this case the plate, made of the same material as the previous annular plate, was 3 mm thick and had an outer radius $a_2 = 0{\cdot}1$ m ($a_1 = 0$).

The experimental modal tests were performed by using an impact excitation. A Brüel & Kjær (B&K) 8202 hammer with mass of 284 g and a steel tip was used. The Frequency Response Functions (FRFs) between 18 excitation points and two response points, located at different radial and angular co-ordinates, were measured. The excitation was applied on a grid with three equidistant points in the radial direction and six positions around the circumference. Both the excitation force and the measured responses were in the axial direction. Two B&K 4393 accelerometers of 2·4 g were employed to measure the plate acceleration. The FRF measurements and the experimental modal parameter estimations were conducted on a HP 9000 workstation with Difa Scadas front-end using the software CADA-X by LMS [58]. The useful frequency ranges up to 3200 Hz with 2 Hz of frequency resolution. The FRFs were estimated by using exponential windows, six averages and the H_V technique [59]; the modal parameters were evaluated by the frequency domain direct parameter estimation method [59]. Due to the very high modal density of the test structure, numerous analyses were performed in order to process together only very few peaks of the FRFs.

Both tanks were tested empty and partially filled with water at five different levels. The maximum filling ratio was $H/a_2 = 1$ for the annular tank and $H/a_2 = 2$ for the circular tank.

6.2. TEST RESULTS AND COMPARISON WITH THE THEORETICAL ONES

Only the first two modes were accurately detected by experiments due to the flexibility of the constraints: the first axisymmetric mode (fundamental mode, $m = 0$ and $n = 0$) and the mode with one nodal diameter and no nodal circles ($m = 1$ and $n = 0$). In fact, it was verified that for higher frequency modes the tank support cannot be considered rigid. The second mode ($m = 1$ and $n = 0$) shows coupled peaks of the FRFs; this is a well-known behaviour of circular and annular plates that is due to the polar symmetry. For each asymmetric mode ($m > 0$) there is a second mode having the same frequency and mode shape but rotated by $\pi/(2m)$. In order to detect the coupled peaks, two references have been used during the tests. The value of the density thickness correction factor is $\mu = 8{\cdot}547$ for the annular plate tested and $\mu = 4{\cdot}245$ for the circular plate.

A comparison of theoretical and experimental results is shown in Figure 9 for the circular plate tested. The theoretical results have been computed by using the NAVMI factors obtained for a simply supported circular plate. These results are practically the same as those obtained by the Rayleigh–Ritz method; in fact the two modes considered do not show internal nodal circles. The results presented in Figure 9 are given as the ratio between the natural frequency with partial water filling and that *in vacuo* (and practically

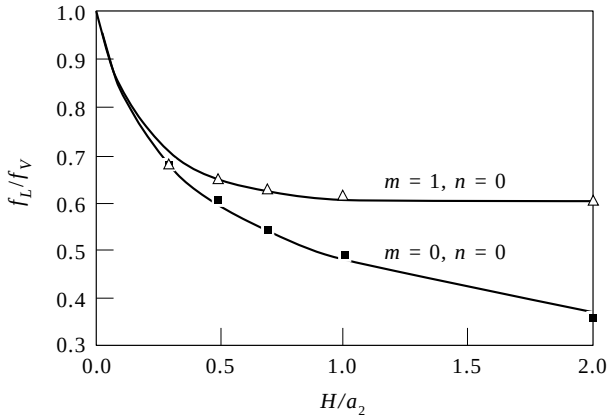

Figure 9. Ratio between the plate natural frequency of the partially water filled tank f_L and of the empty tank f_V versus the filling ratio H/a_2. Comparison of theoretical (solid lines) and experimental (symbols) results. Simply supported circular plate with $\mu = 4{\cdot}245$.

in air). Figure 9 also shows that the larger inertial effect of the water is obtained for the fundamental mode and that the slope of the curves decreases with the filling ratio H/a_2.

In Figure 10, the annular plate tested is considered and the theoretical results have been computed by using the NAVMI factors obtained for an annular plate simply supported outside and free inside; these factors are given in Table 5.

Another interesting phenomenon was observed during the experiments. If the tanks tested are disconnected from the steel support and supported on rubber bands, the natural frequencies of the axisymmetric modes are significantly increased when the tank was filled with water. On the contrary, asymmetric modes are less affected by this change in the constraint. The dynamic behaviour is well justified by the present study. Axisymmetric modes give a movement to the water centre of mass with respect to the tank, so that, if rigid body modes of the tank are allowed, the inertial effect of water on the bottom plate decreases (and frequencies increase). On the contrary, asymmetric modes give no movement to the water center of mass so that rigid body modes do not affect the inertial effect of water to any great extent.

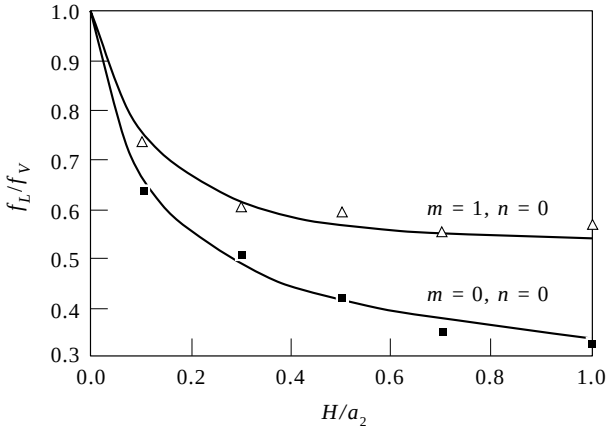

Figure 10. Ratio between the plate natural frequency of the partially water filled tank f_L and of the empty tank f_V versus the filling ratio H/a_2. Comparison of theoretical (solid lines) and experimental (symbols) results. Annular plate simply supported outside and free inside with $a = 0{\cdot}3$ and $\mu = 8{\cdot}547$.

The good agreement between theoretical and experimental results confirms the small influence of free surface waves (neglected in the theory) on bulging modes.

7. CONCLUSIONS

A good agreement has been found between theoretical and experimental results in spite of the difficulty of practically realizing the hypothesized constraints. These results give a validation of the hypotheses and the theory used in the present work. In fact, the hypotheses of inviscid liquid and no cavitation are well verified in the cases tested, when water has been used as liquid inside the tank and small amplitude vibrations have been examined. The effect of the free surface waves is low on bulging modes, as already observed in references [13, 53]. The theory is applicable to engineering problems and the NAVMI factor approach, which estimates well modes without internal nodal circles, has the advantage of presenting the results as tables of non-dimensional factors that can be quickly employed in design. In the case that the entire tank must be considered flexible, however, the approach used is still useful to study the whole structure if a substructuring method, like the artificial spring method, is used [52].

ACKNOWLEDGMENTS

The authors wish to thank Ing. R. Rubini of the Department of Mechanical Engineering (DIEM), University of Bologna, for his helpful assistance during the experiments.

REFERENCES

1. M. K. Au-Yang 1976 *Transactions of the ASME*, *Journal of Applied Mechanics* **43**, 480–484. Free vibration of fluid-filled coaxial cylindrical shells of different lengths.
2. M. K. Au-Yang 1984 *Proceedings of the Conference on Advances in Fluid-Structure Interaction*, *ASME PVP*-78, 17–21 *June*, *San Antonio*, *TX*, 185–203. Dynamics of coupled fluid-shells.
3. H. F. Bauer, J. Siekmann and J. T.-S. Wang 1968 *Journal of Spacecrafts and Rockets* **5**(8), 981–983. Axisymmetric hydroelastic sloshing in an annular cylindrical container.
4. D. Zhou 1994 *Applied Mathematics and Mechanics* **15**(9), 831–839. Free bending vibration of annular cylindrical tank partially filled with liquid in the consideration of surface wave.
5. Y. Kubota and T. Suzuki 1984 *Transactions of the Japan Society of Mechanical Engineers C* **50**, 243–248. Added mass effect on disc vibrating in fluid.
6. M. Amabili, G. Frosali and M. K. Kwak 1996 *Journal of Sound and Vibration* **191**, 825–846. Free vibrations of annular plates coupled with fluids.
7. M. Amabili 1996 *Journal of Sound and Vibration* **193**, 909–925. Effect of finite fluid depth on the hydroelastic vibrations of circular and annular plates.
8. T.-Y. Tsui and N. C. Small 1968 *Journal of Spacecrafts and Rockets* **5**(2), 202–206. Hydroelastic oscillations of a liquid surface in an annular circular cylindrical tank with flexible bottom.
9. H. J.-P. Morand and R. Ohayon 1992 *Interactions Fluides-Structures*. Paris: Masson. See pp. 71–72. (English edition, 1995 *Fluid Structure Interaction*. New York: Wiley).
10. M. K. Kwak and K. C. Kim 1991 *Journal of Sound and Vibration* **146**, 381–389. Axisymmetric vibration of circular plates in contact with fluid.
11. M. K. Kwak 1991 *Transactions of the ASME*, *Journal of Applied Mechanics* **58**, 480–483. Vibration of circular plates in contact with water.
12. M. Amabili and M. K. Kwak 1996 *Journal of Fluids and Structures* **10**, 743–761. Free vibration of circular plates coupled with liquids: revising the "Lamb" problem.
13. M. Amabili 1997 *Shock and Vibration* **4**, 51–68. Bulging modes of circular bottom plates in rigid cylindrical containers filled with a liquid.
14. M. Amabili, G. Dalpiaz and C. Santolini 1995 *Modal Analysis*: *the International Journal of Analytical and Experimental Modal Analysis* **10**, 187–202. Free-edge circular plates vibrating in water.
15. H. Lamb 1921 *Proceedings of the Royal Society* (*London*) **A98**, 205–216. On the vibrations of an elastic plate in contact with water.

16. N. W. McLachlan 1932 *Proceedings of the Physical Society* (*London*) **44**, 546–555. The accession to inertia of flexible discs vibrating in a fluid.
17. W. H. Peake and E. G. Thurston 1954 *Journal of the Acoustical Society of America* **26**(2), 166–168. The lowest resonant frequency of a water-loaded circular plate.
18. P. G. Bhuta and L. R. Koval 1964 *Journal of the Acoustical Society of America* **36**(11), 2071–2079. Hydroelastic solution of the sloshing of a liquid in a cylindrical tank.
19. P. G. Bhuta and L. R. Koval 1964 *Zeitschrift für Angewandte Mathematik und Physik* **15**, 466–480. Coupled oscillations of a liquid with a free surface in a tank.
20. P. Tong 1967 *American Institute of Aeronautics and Astronautics Journal* **5**, 1842–1848. Liquid motion in a circular cylindrical container with a flexible bottom.
21. J. Siekmann and S. C. Chang 1968 *Ingenieur Archiv* **37**, 99–109. On the dynamics of liquid in a cylindrical tank with a flexible bottom.
22. H. F. Bauer, T.-M. Hsu and J. T.-S. Wang 1968 *Transactions of the ASME*, *Journal of Basic Engineering* **90** (Series D, No. 3), 373–377. Interaction of a sloshing liquid with elastic containers.
23. H. F. Bauer, S. S. Chang and J. T.-S. Wang 1971 *American Institute of Aeronautics and Astronautics Journal* **9**, 2333–2339. Nonlinear liquid motion in a longitudinal excited container with elastic bottom.
24. H. F. Bauer and J. Siekmann 1971 *Ingenieur Archiv* **40**, 266–280. Dynamic interaction of a liquid with the elastic structure of a circular cylindrical container.
25. H. F. Bauer, J. T.-S. Wang and P. Y. Chen 1972 *Aeronautical Journal* **76**, 704–712. Axisymmetric hydroelastic sloshing in a circular cylindrical container.
26. G. Muthuveerappan, N. Ganesan and M. A. Veluswami 1979 *Journal of Sound and Vibration* **63**, 385–391. A note on vibration of a cantilever plate immersed in water.
27. D. G. Crighton 1980 *Journal of Sound and Vibration* **68**, 15–33. Approximations to the admittances and free wavenumbers of fluid-loaded panels.
28. H. F. Bauer 1981 *International Journal of Solids and Structures* **17**, 639–652. Hydroelastic vibrations in a rectangular container.
29. D. F. De Santo 1981 *Journal of Pressure Vessel Technology* **103**, 175–182. Added mass and hydrodynamic damping of perforated plates vibrating in water.
30. F. M. Espinosa and A. G. Gallego-Juàrez 1984 *Journal of Sound and Vibration* **94**, 217–222. On the resonance frequencies of water-loaded circular plates.
31. K. Nagaia and J. Takeuchi 1984 *Journal of the Acoustical Society of America* **75**(5), 1511–1518. Vibration of a plate with arbitrary shape in contact with a fluid.
32. K. Nagaia and K. Nagai 1986 *Journal of Sound and Vibration* **70**, 333–345. Dynamic response of circular plates in contact with a fluid subjected to general dynamic pressures on a fluid surface.
33. Y. Fu and W. G. Price 1987 *Journal of Sound and Vibration* **118**, 495–513. Interactions between a partially or totally immersed vibrating cantilever plate and the surrounding fluid.
34. H. F. Bauer and W. Eidel 1988 *Journal of Sound and Vibration* **125**, 93–114. Non-linear hydroelastic vibrations in rectangular containers.
35. P. Capodanno 1989 *Revue Roumaine des Sciences Techniques—Série de Mécanique Appliquée* **34**(3), 241–266. Vibrations d'un liquide dans un vase fermé par une plaque èlastique.
36. J. H. Ginsberg and P. Chu 1992 *Journal of the Acoustical Society of America* **91**(2), 894–906. Asymmetric vibration of a heavily fluid-loaded circular plate using variational principles.
37. M. Chiba 1992 *Journal of Fluids and Structures* **6**, 181–206. Nonlinear hydroelastic vibration of a cylindrical tank with an elastic bottom, containing liquid. Part I: experiment.
38. M. Chiba 1993 *Journal of Fluids and Structures* **7**, 57–73. Nonlinear hydroelastic vibration of a cylindrical tank with an elastic bottom, containing liquid. Part II: linear axisymmetric vibration analysis.
39. M. Chiba 1994 *Journal of Sound and Vibration* **169**, 387–394. Axisymmetric free hydroelastic vibration of a flexural bottom plate in a cylindrical tank supported on an elastic foundation.
40. S. M. Soedel and W. Soedel *Journal of Sound and Vibration* **171**, 159–171. On the free and forced vibration of a plate supporting a freely sloshing surface liquid.
41. P. Hagedorn 1994 *Journal of Sound and Vibration* **175**, 233–240. A note on the vibrations of infinite elastic plates in contact with water.
42. M. K. Kwak 1994 *Journal of Sound and Vibration* **178**, 688–690. Vibration of circular membranes in contact with water.
43. M. Amabili 1994 *Proceedings of the First International Conference on Vibration Measurements by Laser Techniques*: *Advances and Applications*, 3–5 *October*, *Ancona*, *Italy*, 421–429. Modal properties of annular plates vibration in water.

44. H. F. BAUER 1995 *Journal of Sound and Vibration* **180**, 689–704. Coupled frequencies of a liquid in a circular cylindrical container with elastic liquid surface cover.
45. J. H. GINSBERG, K. CUNEFARE and H. PHAM 1995 *Transactions of the ASME*, *Journal of Vibration and Acoustics* **117**, 206–212. A spectral description of inertial effects in fluid-loaded plates.
46. F. ZHU 1994 *Journal of Sound and Vibration* **171**, 641–649. Rayleigh quotients for coupled free vibrations.
47. M. AMABILI 1995 *Journal of Sound and Vibration* **180**, 526. Comments on "Rayleigh quotients for coupled free vibrations".
48. F. ZHU 1995 *Journal of Sound and Vibration* **186**, 543–550. Rayleigh–Ritz method in coupled fluid-structure interacting systems and its applications.
49. A. W. LEISSA 1969 *Vibration of Plates*, *NASA SP*-160. Washington, DC: Government Printing Office.
50. R. V. SOUTHWELL 1922 *Proceedings of the Royal Society* (*London*) **101**, 133–153. On the free transverse vibrations of uniform circular disc clamped at its center; and on the effects of rotation.
51. S. M. VOGEL and D. W. SKINNER 1965 *Transactions of the ASME*, *Journal of Applied Mechanics* **32**, 926–931. Natural frequencies of transversely vibrating uniform annular plates.
52. M. AMABILI 1997 *Journal of Sound and Vibration* **199**, 431–452. Shell–plate interaction in the free vibrations of circular cylindrical tanks partially filled with a liquid: the artificial spring method.
53. H. KONDO 1981 *Bulletin of the Japan Society of Mechanical Engineers* **24**, 215–221. Axisymmetric vibration analysis of a circular cylindrical tank.
54. H. LAMB 1945 *Hydrodynamics*. New York: Dover. See p. 46.
55. L. MEIROVITCH 1986 *Elements of Vibration Analysis*, (second edition). New York: McGraw-Hill. See pp. 270–282.
56. S. WOLFRAM 1991 *Mathematica*: *A System for Doing Mathematica by Computer* (second edition). Redwood, CA: Addison-Wesley.
57. D. J. GUNARATNAM and A. P. BHATTACHARYA 1985 *Journal of Sound and Vibration* **102**, 431–439. Transverse vibration of circular plates having mixed elastic rotational edge restraints and subjected to in-plane forces.
58. *Cada Modal/Analysis User Manual*. Leuven, Belgium: LMS.
59. P. Sas (editor) 1993 *Course on Modal Analysis Theory and Practice* (*Proceedings of the* 18*th International Seminar on Modal Analysis*). Leuven. Belgium: Katholieke Universiteit.

APPENDIX: ORTHOGONALITY OF FUNCTIONS F_m

The orthogonality of the functions F_m given in equation (18) is proved as follows. The functions F_m are defined in equation (16). It is supposed that $k \neq h$; for brevity, one denotes

$$W_k = F_m(\epsilon_{mk}\rho), \qquad W_h = F_m(\epsilon_{mh}\rho). \tag{A1, A2}$$

The functions W_k and W_h are solutions of the Bessel equations

$$\rho^2 W_k'' + \rho W_k' + (\epsilon_{mk}^2\rho^2 - m^2)W_k = 0, \qquad \rho^2 W_h'' + \rho W_h' + (\epsilon_{mh}^2\rho^2 - m^2)W_h = 0. \tag{A3, A4}$$

If one multiplies equations (A3) and (A4) by W_h and W_k, respectively, and then sums up, the result is

$$\rho^2(W_h W_k'' - W_k W_h'') + \rho(W_h W_k' - W_k W_h') = (\epsilon_{mh}^2 - \epsilon_{mk}^2)\rho^2 W_h W_k. \tag{A5}$$

Dividing equation (A5) by ρ, one obtains

$$(\mathrm{d}/\mathrm{d}\rho)[\rho(W_h W_k' - W_k W_h')] = (\epsilon_{mh}^2 - \epsilon_{mk}^2)\rho W_h W_k. \tag{A6}$$

Using equations (A1) and (A2), one obtains the proof:

$$(\epsilon_{mh}^2 - \epsilon_{mk}^2)\int_a^1 \rho F_m(\epsilon_{mk}\rho)F_m(\epsilon_{mh}\rho)\mathrm{d}\rho = \rho[F_m(\epsilon_{mh}\rho)F_m'(\epsilon_{mk}\rho) - F_m(\epsilon_{mk}\rho)F_m'(\epsilon_{mh}\rho)]|_a^1 = 0, \tag{A7}$$

here the condition that ϵ_{mk} and ϵ_{mh} are different roots of equation (17) has been used.